The broken-symmetry phase of solid hydrogen: evidence from infrared and Raman active vibrons

2007 J. Phys.: Condens. Matter 19 425237

(http://iopscience.iop.org/0953-8984/19/42/425237)

IOP PUBLISHING JOURNAL OF PHYSICS: CONDENSED MATTER

J. Phys.: Condens. Matter **19** (2007) 425237 (9pp) doi:10.1088/0953-8984/19/42/425237

The broken-symmetry phase of solid hydrogen: evidence from infrared and Raman active vibrons

L J Zhang, Y L Niu, T Cui, Y Li, Y M Ma[1], Z He and G T Zou[1]

National Laboratory of Superhard Materials, Jilin University, Changchun 130012, People's Republic of China

E-mail: mym@jlu.edu.cn and gtzou@jlu.edu.cn

Received 3 August 2007
Published 18 September 2007
Online at stacks.iop.org/JPhysCM/19/425237

Abstract

The infrared (IR) and Raman-active vibrons (intramolecular stretching modes) of solid hydrogen in the broken-symmetry phase (phase II) are extensively studied using density-functional linear-response theory. We performed a group-theoretical analysis of allowed IR and Raman vibrons for proposed candidate structures to aid in determining the structure of phase II. From a comparison of the calculated intensities and frequencies of IR and Raman vibrons with available experimental results, some structures have been excluded. The current theory indicated that phase II of solid hydrogen might have the recently suggested incommensurate structure with *Pa*3-type local orientational order for solid deuterium, and that the energetically preferred $P2_1/c$ structure is also a better candidate.

1. Introduction

Since the classic study by Wigner and Huntington [1], a wealth of information about the phase diagram of hydrogen at high pressures has been collected. Experimentally, solid hydrogen remains a low-temperature quantum molecular solid up to very high pressures ($P < 110$ GPa). Upon compression, electric quadrupole–quadrupole interactions lead to a broken-symmetry phase transition, in which the molecules go from a spherical rotational state to an anisotropic rotational state [2]. Very recently, Goncharenko *et al* [3][2] successfully performed x-ray and neutron diffraction measurements up to 60 GPa in solid deuterium. They suggested that phase II of solid deuterium is an incommensurate structure with *Pa*3-type local orientational order. However, in solid hydrogen a complete understanding of the structural properties of phase II by experiments is not yet available, due to the well-known problem of hydrogen's weak diffraction intensity [2]. By considering that the structure of phase II could depend on the isotope [4],

[1] Authors to whom any correspondence should be addressed.

[2] In the paper, the proposed *Pa*3 local order of the incommensurate structure has been presented in $P\bar{3}$ symmetry. However, we found that the proposed structure has $P\bar{3}m1$ symmetry. Actually it can be described in both space groups (private communication with Goncharenko).

whether the structure in phase II for solid hydrogen also has an incommensurate structure with *Pa*3 local order is, thus, not known conclusively. On the theoretical side, various candidate structures for phase II of solid hydrogen have been proposed based on density-functional theory (DFT) ($Cmc2_1$ [5, 7], $Pca2_1$ [6–10], and $P2_1/c$ [11]) and path-integral Monte Carlo simulation (*Pa*3-type local [12, 13]); however, the elucidation of the structure is still under debate [14].

The only well-documented experiments for phase II of solid hydrogen are Raman and infrared (IR) measurements. Optical measurements in phase II of solid hydrogen indicated the presence of two IR active vibrons, in contrast to phase I, where only one is observed. Raman spectra in phase II show a single peak at lower frequency than that of the IR modes, and the frequency decreases upon compression [2]. A number of theoretical studies on vibrons have appeared [6–8, 10, 15–19]; however, all the studies are limited to frequency calculations, while not taking the peak intensity into account. We have to emphasize that due to the perturbation by the background and noise, real measurements might not detect specific peaks with very weak intensities [20]. Thus, the theoretical Raman or IR intensity is expected to play an important role in interpreting the experimental measurements. Consequently, more extensive theoretical studies on the vibrons by explicitly including the intensity calculations are needed to fully understand the experimental Raman and IR spectra and, thus, could help to determine the structure and molecular orientations of phase II.

2. Computational details

Ab initio calculations were carried out using the plane-wave pseudopotential method within the framework of density-functional theory (DFT) [21]. We calculated the phonon frequencies based on the linear-response method [22]. In this approach, the dynamical matrix is expressed in terms of the inverse dielectric matrix describing the response of the valence electron density to a periodic lattice perturbation. The generalized gradient approximation (GGA) of the exchange–correlation functional [23] is used in the calculations. The Troullier–Martins (TM) norm-conserving scheme [24] is used to generate the pseudopotential for H with a matching radius of 0.6 au. Particular attention was paid to generate a reliable hard hydrogen pseudopotential for calculations at high pressures. We used an 80 Ryd cutoff of the kinetic energy of the plane waves and a self-consistent field tolerance of 1.0×10^{-8} Ryd/unit cell in all calculations. The candidate structures in this study are previously theoretical proposed structures with space group $P6_3/mmc$(m-*hcp*), $Pca2_1$, $Cmc2_1$, $P2_1/c$, and $Cmca$ [2, 14] The recently proposed *Pa*3 local order of the incommensurate structure by Goncharenko *et al* [3] (see footnote 2) can be mimicked by a unit cell of $P\bar{3}m1$ symmetry containing eight hydrogen molecules. Note that in their works, the neutron diffraction intensities of the periodic structure containing the characteristics of the *Pa*3 local order are calculated and seen to be in good agreement with experiments. It should be pointed out that the vibrons give a direct intramolecular vibration description of the structure; thus, they reflect mainly the information on the short-range local behaviour. To probe the short-range local nature of phase II, therefore, it is appropriate to study, instead of the incommensurate structure, the periodic $P\bar{3}m1$ structure. We generate the k-point grids via the Monkhorst–Pack scheme [25] for the electronic Brillouin zone (BZ) integration. The k-point sampling used in our calculations was $16 \times 16 \times 10$ (m-*hcp*), $10 \times 16 \times 10$ ($Pca2_1$), $16 \times 16 \times 10$ ($Cmc2_1$), $10 \times 10 \times 16$ ($P2_1/c$), $16 \times 16 \times 10$ ($Cmca$), and $12 \times 12 \times 12$ ($P\bar{3}m1$), which proved to be sufficient in the present studies. In phonon calculations, these choices are found to yield frequencies that converge to within 0.05 THz for all the structures.

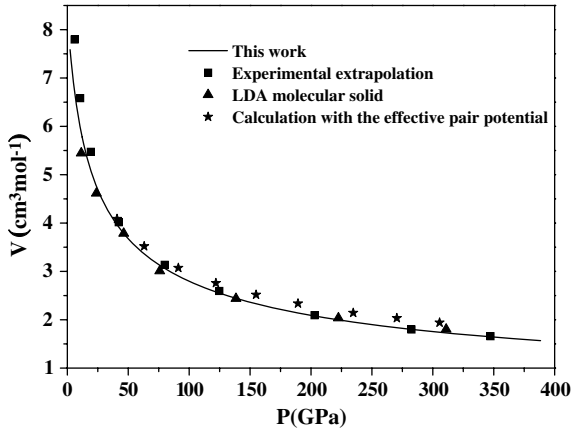

Figure 1. Comparison of the calculated equation of state (EOS) with other calculations and experiment. The solid line is our results. The solid triangles are local-density approximation (LDA) calculations including zero-point motion in the quasiharmonic approximation [30]. The solid stars are calculated with the effective pair potential [31]. The solid squares are data from the experimental extrapolation [29].

3. Results and discussions

To test the choice of the TM pseudopotential and the GGA approximation in this study, we first performed the equation of state (EOS) calculations for solid molecular hydrogen. The EOS is calculated over a wide pressure range (including phase I, II, and III) with the m-*hcp* structure, in which the axes of all molecules are aligned parallel to *c*, although this structure has been proved to be energetically unstable [14]. However, it is noteworthy that the m-*hcp* structure represents the general features of the hexagonal close-packed lattice among candidate structures. With consideration of the small energy differences in these structures, regardless of molecular orientations [26] (see also figure 2), it has been verified that the theoretical EOS is nearly the same among the candidate structures by our theoretical calculation (not shown) and our previous work [27]. Moreover, for comparison, the choice of the m-*hcp* structure in the EOS calculation also takes advantage of other existing theoretical data. The cell parameters and the bond lengths are optimized at selected pressures in the m-*hcp* structure and the total energies are fitted as a function of volume to the Murnaghan EOS [28]. In figure 1, the calculated EOS (solid line) is compared with experimental results [29] (solid squares) and two previous theoretical calculations [30, 31] (solid triangles and stars). It is clear that our calculations are in excellent agreement with the EOS data extrapolated from experiments and the previous theoretical results. Thus, these comparisons strongly support the choice of our pseudopotentials and the GGA approximation for other hydrogen systems at high pressures. Note that the calculated EOS does not include the quantum anharmonic effects in the free rotational state of phase I and therefore might not be valid for the low-pressure range. The slight disagreement with experimental results at low pressures also might be dominated by the GGA approximation within DFT employed here.

We investigated the energetics of the candidate structures with space group $P6_3/mmc$(m-*hcp*), $Pca2_1$, $Cmc2_1$, $P2_1/c$, $Cmca$, and $P\bar{3}m1$, respectively, for phase II of solid hydrogen through total-energy calculations. With regards to the zero-point energy (ZPE), Surh *et al* have shown that introduction of it by adding the contribution of selected

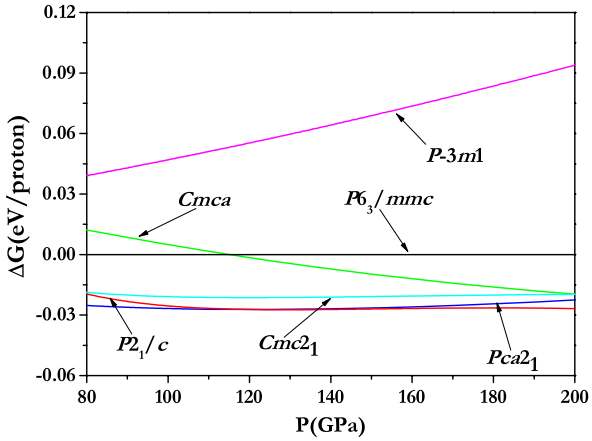

Figure 2. Gibbs free-energy curves (relative to the m-*hcp* ($P6_3/mmc$)) structure as a function of pressure for solid molecular hydrogen.

(This figure is in colour only in the electronic version)

phonon modes may affect the stability of competing low-pressure phases [15]. However, for orientationally ordered phases at high pressures, the effect of ZPE on the molecular orientation and the transition pressures might not be severe [17, 32]. In contrast, the rotational spectra in phase II indicate that the rotational state of the molecules is much closer to a quantum free rotor than to a classical motion around a well-defined molecular orientation [33]. From their results, the ZPE is likely to be very important, even in the orientationally ordered phases. Apparently, the situation on the ZPE is extremely complex, and this is still an open question. However, it is at present difficult to include the ZPE within the first-principles calculation and perform a rigorous quantum-mechanics calculation. Thus, we have not taken the ZPE into account here. For each structure we fully optimized the bond lengths, molecular orientations and cell parameters at each density. For the $P\bar{3}m1$ structure, we found that full optimization will lead to the axes of all molecules being aligned parallel to c-axis (similar to the m-*hcp* structure), which is a serious deviation from the *Pa*3-type local order. In order to keep the *Pa*3 local order, we have to reduce the convergence threshold on forces to 1.0×10^{-2} Ryd/au (in other structures, the value is 1.0×10^{-3} Ryd/au). The free-energy difference among the candidate structures is presented in figure 2. We find that the energy of the $P\bar{3}m1$ structure is the highest among the selected structures. From the calculated electronic band structures (not shown), it is found that the band gaps in the $P\bar{3}m1$ structure closed at about 110 GPa, in contradiction with the fact that solid hydrogen is an insulator in phase II. The calculated periodic, instead of incommensurate, structure of *Pa*3-type local order might be responsible for this discrepancy. There are no stable regions for the $Cmc2_1$ and *Cmca* structures which are energetically unfavoured. It should be pointed out that the $P2_1/c$ structure, slightly lower than $Pca2_1$, is found to be the most energetically favoured structure among the candidate structures in the pressure range of phase II, in agreement with the previous *ab initio* calculations [11].

A satisfactory structure for phase II of solid hydrogen would be compatible with optical measurements on vibrons, where a strong Raman peak and two IR modes are observed [2]. With the linear-response theory we can calculate the zone-centre (Γ) phonon frequencies, eigenvectors, and the dynamical matrix D (Γ). The group theory analysis allows us to decompose the matrix D (Γ) into blocks, each of them corresponding to an irreducible

Table 1. The group theoretically allowed IR and Raman active vibrons corresponding to proposed candidate structures for solid molecular hydrogen.

Space group	IR vibron	Raman vibron
$P6_3/mmc$(m-*hcp*)[a]		A_{1g}
$P2_1/c$	$A_u + B_u$	$A_g + B_g$
$Pca2_1$	$A_1 + B_1 + B_2$	$A_1 + A_2 + B_1 + B_2$
$P\bar{3}m1$(*Pa*3-local)	$2A_{2u} + E_u$	$2A_{1g} + E_g$
$Cmc2_1$	$A_1 + B_2$	$A_1 + B_2$
Cmca[a]		$A_{1g} + B_{3g}$

[a] Reference [10].

representation of the Γ-group. The irreducible representations of allowed IR and Raman active vibrons are given in table 1. Since the m-*hcp* and *Cmca* structures do not allow the experimentally observed IR vibron activity, we can rigorously rule out these two structures. For other candidate structures, there exist more allowed IR and Raman active vibrons than experimental observation. However, we still keep them in the list of candidate structures for phase II by considering that some of vibrons might be too weak to be experimentally observed due to signal-to-noise considerations. Therefore calculations of relative intensity are urgently required to aid in determining the structure and molecular orientations for phase II.

IR intensity calculations are performed through the calculations of Born effective charge tensors Z^* [34]. Raman intensities are computed from the second-order derivative of the electronic density matrix with respect to a uniform electric field [35]. In a Raman spectrum the peak intensity I^ν corresponding to an optical phonon ω_ν can be computed as

$$I^\nu \propto |e_i \overleftrightarrow{A}^\nu \cdot e_s|^2 \frac{1}{\omega_\nu} (n_\nu + 1), \tag{1}$$

where $e_i(e_s)$ is the polarization of the incident (scattered) radiation, $n_\nu = [\exp(\hbar\omega/k_B T) - 1]^{-1}$, and

$$A^\nu_{lm} = \sum_{k\gamma} \frac{\partial^3 \varepsilon^{el}}{\partial E_l \partial E_m \partial u_{k\gamma}} \frac{w^\nu_{k\gamma}}{\sqrt{M_\gamma}} \tag{2}$$

where ε^{el} is the electronic energy of the system, E_l is the lth Cartesian component of a uniform electric field, $u_{k\gamma}$ is the displacement of the γth atom in the kth direction, M_γ is the atomic mass, and $w^\nu_{k\gamma}$ is the orthonormal vibrational eigenmode ν. According to the Hellmann–Feynman theorem,

$$\frac{\partial^3 \varepsilon^{el}}{\partial E_l \partial E_m \partial u_{k\gamma}} = 2\,\mathrm{Tr}\left\{ \left(\frac{\partial^2 \rho}{\partial E_l \partial E_m} \right) \frac{\partial V^{ext}}{\partial u_{k\gamma}} \right\}, \tag{3}$$

where the DFT density matrix $\rho = \sum_\nu |\psi_\nu\rangle\langle\psi_\nu|$, $\langle\psi_\nu|$ being the normalized occupied Kohn–Sham (KS) eigenstates, $\mathrm{Tr}\{O\}$ is the trace of the operator O, and V^{ext} is the external ionic potential.

In figures 3(a), (b), (c) and (d) we present relative intensity calculations of IR and Raman vibrons for the candidate $Cmc2_1$, $Pca2_1$, $P\bar{3}m1$, and $P2_1/c$ structures, respectively. All the calculations are performed at 130 GPa, which is in the pressure range of phase II. For the $Cmc2_1$ and $Pca2_1$ structures shown in figures 3(a) and (b), the A_1 vibron with strong intensities for both structures are both IR and Raman active modes, in contradiction with experimental measurements in which the IR and Raman peaks have different frequencies. Therefore, we can confidently eliminate the choice of $Cmc2_1$ and $Pca2_1$ structures in phase II.

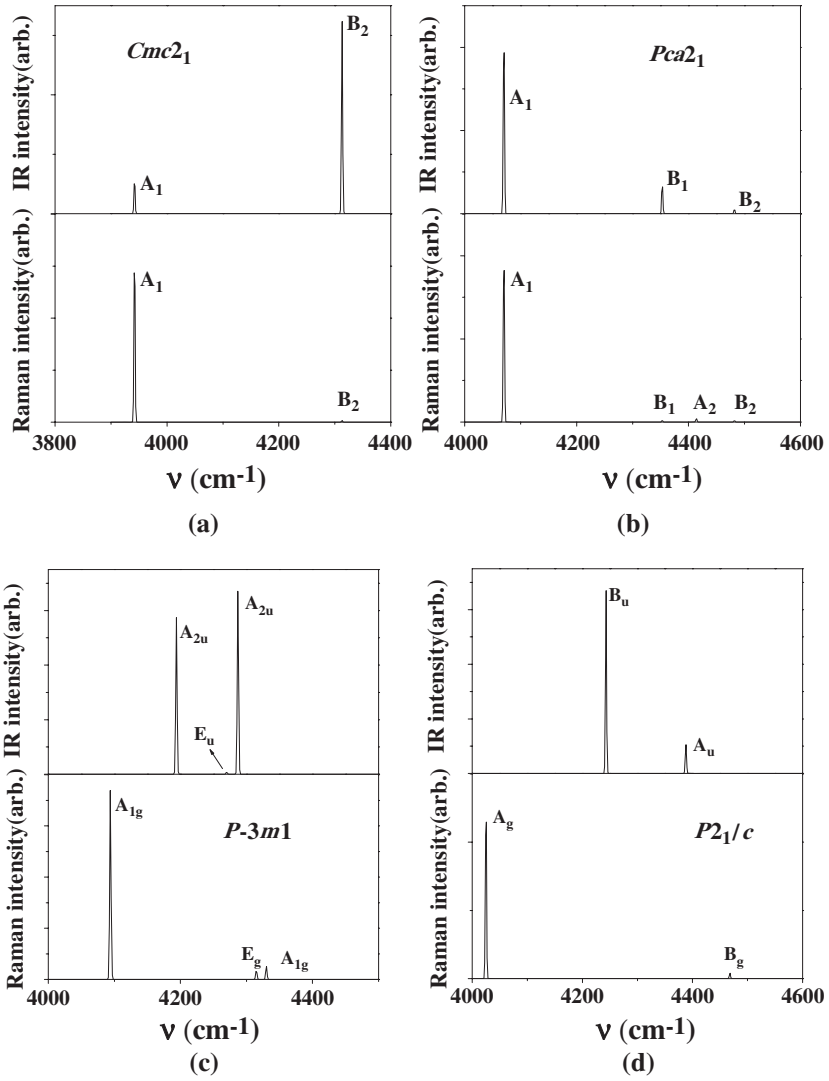

Figure 3. Calculated intensities of the IR and Raman active vibrons for solid molecular hydrogen with the $Cmc2_1$ (a), $Pca2_1$ (b), $P\bar{3}m1$ (c), $P2_1/c$ (d) structure at 130 GPa, respectively.

For the $P\bar{3}m1$ structure, the phonon calculations at the zone centre show large negative values in the optical branches, indicating that the $P\bar{3}m1$ structure is dynamically unstable. However, this might also be attributed to the currently calculated periodic, instead of incommensurate, structure of *Pa*3-type local orientational order. As shown in figure 3(c), there are eight vibrons (labelled as two A_{1g}, two A_{2u}, E_g, and E_u respectively); four of them (two A_{1g}, and E_g) are Raman active, and four of them (two A_{2u}, and E_u) IR active. One observes that there exist two extremely strong IR active modes (both A_{2u} modes) and one extremely strong Raman mode (A_{1g}), in apparent agreement with the experimental IR and Raman spectrum. The other three modes with very weak intensities (E_u, the other A_{1g}, and E_g) might not be experimentally observed, when taking signal-to-noise effects into account [20]. In figure 4(a), we report the

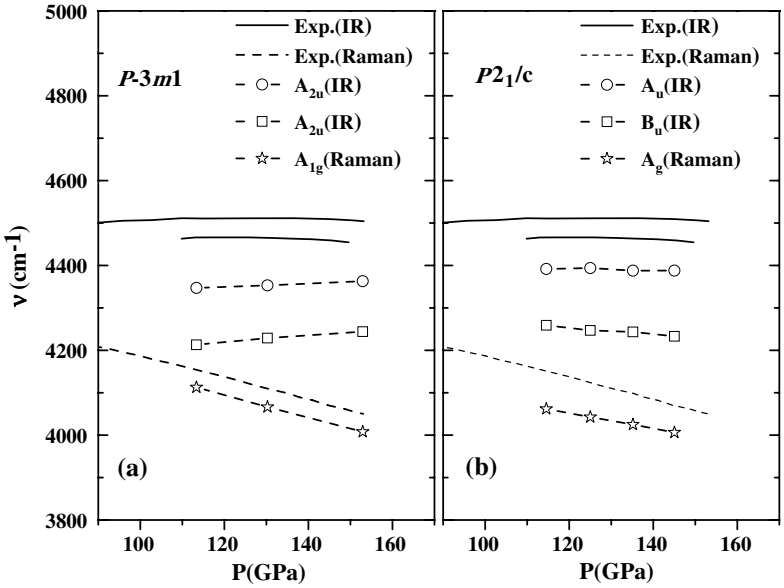

Figure 4. (a) The calculated vibron frequencies of solid hydrogen with the $P\bar{3}m1$ structure as a function of pressure. The lower line and the couple of upper solid lines are experimental Raman and IR data, respectively [2]. Open circles and squares are calculated stronger IR active vibrons (both modes A_{2u}). Open stars are the strongest calculated Raman active vibrons (mode A_{1g}); see also figure 3(c). (b) The calculated vibron frequencies of solid hydrogen with the $P2_1/c$ structure as a function of pressure. Solid lines are experimental data. Open circles and squares are calculated IR active vibrons (modes A_u and B_u). Open stars are the stronger calculated Raman active vibrons (mode A_g); see also figure 3(d).

calculated frequencies of vibrons with pressure for the $P\bar{3}m1$ structure[3]. In order to compare with the experimental data (solid and dashed lines), we present only one strong Raman mode (open stars) and two strong IR modes (open circles and squares). The Raman mode (A_{1g}) obviously decreases with pressure, and the pressure dependences of the two IR modes (both A_{2u} modes) show an almost flat trend, which both agree with experimental results. Generally, with the exception of higher frequencies, the $P\bar{3}m1$ structure gives a reasonable description (the relative intensities and pressure dependence) of the experimental observation of IR and Raman active vibrons for phase II, based on the current theoretical model.

The intensities of IR and Raman vibrons for the $P2_1/c$ structure are shown in figure 3(d). In this structure there exist four vibrons (labelled as A_u, B_u, A_g, and B_g respectively); two of them (A_g and B_g) are Raman active, and the other two (A_u and B_u) are IR active. The Raman mode A_g is much stronger than B_g, which is consistent with the experimental results. The IR modes A_u and B_u show large intensities; thus, they should be strong enough to be experimentally observed, in a good agreement with experimental measurements. We also present the calculated frequencies of vibrons with pressure for the $P2_1/c$ structure in figure 4(b). Note that the Raman mode B_g is not plotted, due to its very weak intensity. It is found that all theoretical frequencies (open symbols) are slightly lower than experimental data

[3] In order to keep the $P\bar{3}m1$ symmetry, partial relaxation (as explained above) was found to be necessary to obtain the structure parameters at different pressures. After optimization it was found that the $P\bar{3}m1$ structure contains molecules with the longer and shorter bonds, and that the bond lengths decrease drastically, which leads to high vibron frequencies. A constant downward shift of 320 cm^{-1} has been added to all frequencies in order to compare with the experimental data. It should be pointed out that this *ad hoc* correction does not change any physical meanings.

(solid and dash lines), which might be attributed to the longer bond lengths for this structure in our theoretical simulations. Note that the lower IR mode B_u (open squares) has a higher frequency than the Raman mode A_g (open stars) with the frequency difference $\sim$240 cm^{-1} at about 110 GPa. This difference is in reasonable agreement with the experimentally observed value, $\sim$300 cm^{-1}, between the upper IR vibron and the Raman mode, at the same pressure. However the frequency difference between the two IR modes (open circles and squares) is apparently larger than the experimental value. It is clearly found that the IR modes are almost flat and the Raman mode obviously decreases with pressure, in excellent agreement with experimental results. The calculated electronic band structures for the $P2_1/c$ structure (not shown) suggested that this structure still remains an insulator with a large energy gap of 2.4 eV when the pressure increases up to 150 GPa. This fact is also consistent with the experimental measurements that no sign of metallization appears in the pressure range of phase II [2].

It should be pointed out that the calculations might give different results if we take the ortho–para distinction [36] of solid hydrogen into account. However, our method employed here could not deal with such states or systems. In our recent previous work through extensively lattice dynamics calculations, it has been reported that the $Pca2_1$ structure is a good candidate for phase II, while the $P2_1/c$ structure shows dynamical instability by evidencing a softening mode at the zone boundary B point [27]. These conclusions are obviously incompatible with the present results based on calculations of IR and Raman active vibrons. Thus, the solid hydrogen problem turns out to be extremely complicated, and still remains open. We should also emphasize that a full understanding of the lattice dynamics of solid hydrogen may require consideration of anharmonic effects on the vibrations. The increasing anharmonicity with pressure might shift slightly the frequencies of the vibron modes [2, 37]. However, recent Raman measurements of molecular hydrogen under simultaneous conditions of high temperature and high static pressure implied that the anharmonicity decreases with pressure [38]. Therefore our linear-response calculations in the frame of the harmonic approximation might be a reasonable assumption at high pressures. In principle, the frozen-phonon approach can be used to include anharmonic effects but such calculations are beyond the scope of this study.

4. Conclusion

In summary, by means of density-functional linear-response theory, the IR and Raman active vibrons of solid hydrogen in the broken-symmetry phase have been extensively studied. To narrow down the possible structures, we have performed a group-theoretical analysis of allowed IR and Raman active vibrons for proposed candidate structures. In the frame of the harmonic approximation, we calculated both the frequencies and relative intensities of IR and Raman active vibrons. From comparison with experimental observations some structures have been rigorously ruled out. We have shown, first, the Raman and IR evidence for the recently proposed *Pa*3-type local orientational order of the incommensurate structure [3] (see footnote 2). Therefore the broken-symmetry phase of solid hydrogen might also have the recently suggested incommensurate structure with *Pa*3-type local orientational order. From the results of calculated energetics, band structure, and the IR and Raman active vibrons, the $P2_1/c$ structure is also a good candidate.

Acknowledgments

We thank I Goncharenko for valuable discussions. This work is supported by the National Nature Science Associate Foundation of China (No. 10676011), the China 973

Program (No. 2005CB724400), the National Basic Research Priorities Program of China (No. 2001CB711201), the Key Research Program of Education Ministry of China (No. 03057), the National Doctoral Foundation of China Education Ministry (No. 20050183062), the Scientific Research Foundation for the Returned Overseas Chinese Scholars, State Education Ministry the Program for 2005 New Century Excellent Talents in University, and the 2006 Project for Scientific and Technical Development of Jilin Province. Calculations in this work have been done using the Quantum-ESPRESSO package [39].

References

[1] Wigner E and Huntington H B 1935 *J. Chem. Phys.* **3** 764
[2] Mao H K and Hemley R J 1994 *Rev. Mod. Phys.* **66** 671 and references therein
[3] Goncharenko I and Loubeyre P 2005 *Nature* **435** 1206
[4] Goncharov A F, Hemley R J, Mao H K and Shu J 1998 *Phys. Rev. Lett.* **80** 101
[5] Kitamura H, Tsuneyuki S, Ogitus T and Miyake T 2000 *Nature* **404** 259
[6] Kohanoff J, Scandolo S, Chiarotti G L and Tosatti E 1997 *Phys. Rev. Lett.* **78** 2783
[7] Nagao K and Nagara H 1998 *Phys. Rev. Lett.* **80** 548
[8] Nagao K, Takezawa T and Nagara H 1999 *Phys. Rev.* B **59** 13741
[9] Stadele M and Martin R M 2000 *Phys. Rev. Lett.* **84** 6070
[10] Cui L, Chen N H and Silvera I F 1995 *Phys. Rev.* B **51** 14987
[11] Johnson K A and Ashcroft N W 2000 *Nature* **403** 632
[12] Cui T, Cheng E, Alder B J and Whaley K B 1997 *Phys. Rev.* B **55** 12253
[13] Kaxiras E and Guo Z 1994 *Phys. Rev.* B **49** 11822
[14] Maksimov E G and Shilov Y I 1999 *Phys.—Usp.* **42** 1121 and references therein
[15] Surh M P, Barbee T W III and Mailhiot C 1993 *Phys. Rev. Lett.* **70** 4090
[16] Eggert J H, Mao H K and Hemley R J 1993 *Phys. Rev. Lett.* **70** 2301
[17] Tse J S and Klug D D 1995 *Nature* **378** 595
[18] Scheerboom M I M and Schouten J A 1996 *Phys. Rev.* B **53** R14705
[19] Cui L, Chen N H and Silvera I F 1998 *Phys. Rev.* B **57** 656 (erratum)
[20] McCreery R L 2000 *Raman Spectroscopy for Chemical Analysis* (New York: Wiley) chapter 2
[21] Hohenberg P and Kohn W 1964 *Phys. Rev.* **136** B864
Kohn W and Sham L J 1965 *Phys. Rev.* **140** A1133
[22] Baroni S, Giannozzi P and Testa A 1987 *Phys. Rev. Lett.* **58** 1861
Giannozzi P, de Gironcoli S, Pavone P and Baroni S 1991 *Phys. Rev.* B **43** 7231
[23] Perdew J P and Burke K 1996 *Int. J. Quantum Chem.* S **57** 309
Perdew J P, Burke K and Ernzerhof M 1996 *Phys. Rev. Lett.* **77** 3865
[24] Troullier N and Martins J L 1991 *Phys. Rev.* B **43** 1993
[25] Monkhorst H J and Pack J D 1976 *Phys. Rev.* B **13** 5188
[26] Nagao K, Nagara H and Matsubara S 1997 *Phys. Rev.* B **56** 2295
[27] Zhang L J, Niu Y L, Cui T, Li Y, Wang Y, Ma Y M, He Z and Zou G T 2006 *J. Phys.: Condens. Matter* **18** 9917
[28] Murnaghan F D 1944 *Proc. Natl Acad. Sci. USA* **30** 244
[29] Loubeyre P, Letoullec R, Hausermann D, Hanfland M, Hemley R J, Mao H K and Finger L W 1996 *Nature* **383** 702
[30] Barbee T W III, Garcia A and Cohen M L 1989 *Phys. Rev. Lett.* **62** 1150
[31] Duffy T S, Vos W L, Zha C S, Hemley R J and Mao H K 1994 *Science* **263** 1590
[32] Natoli V, Martin R M and Ceperley D 1995 *Phys. Rev. Lett.* **74** 1601
[33] Mazin I I, Hemley R J, Goncharov A F, Hanfland M and Mao H K 1997 *Phys. Rev. Lett.* **78** 1066
[34] Baroni S, de Gironcoli S, Corso A and Giannozzi P 2001 *Rev. Mod. Phys.* **73** 515
[35] Lazzeri M and Mauri F 2003 *Phys. Rev. Lett.* **90** 036401
[36] Silvera I F 1980 *Rev. Mod. Phys.* **52** 393
[37] Ashcroft N W 1990 *Phys. Rev.* B **41** 10963
[38] Goncharov A F and Crowhurst J C 2006 *Phys. Rev. Lett.* **96** 055504
[39] Baroni S, Dal Corso A, de Gironcoli S, Giannozzi P, Cavazzoni C, Ballabio G, Scandolo S, Chiarotti G, Focher P, Pasquarello A, Laasonen K, Trave A, Car R, Marzari N and Kokalj A http://www.pwscf.org/